# Photocatalytic Properties of TiO$_2$ Nanotubes Doped with Ag, Au and Pt or Covered by Ag, Au and Pt Nanodots

**Mihail Enachi[a], Maria Guix[b], Tudor Braniste[a], Vitalie Postolache[a], Vladimir Ciobanu[a], Veaceslav Ursaki[c], Oliver G. Schmidt[b], Ion Tiginyanu[a,c]**

*[a]National Center for Material Study and Testing,
Technical University of Moldova,
Stefan cel Mare, av. 168, MD-2004, Chisinau, Republic of Moldova
[b]Institute for Integrative Nanoscience,
Leibniz Institute for Solid State and Materials Research (IFW), D-01171, Dresden, Germany
[c]Institute of Electronic Engineering and Nanotechnologies, Academy of Science of Moldova,
Academiei, str., 3/3, MD-2028, Chisinau, Republic of Moldova*

Titania nanotube arrays have been prepared by anodic oxidation of titanium foils in an electrolyte solution containing a mixture of hydrofluoric acid, ethylene glycol, and phosphoric acid. The initially amorphous nanotubes were found to crystalize in an anatase phase upon thermal treatment at 500°C. Anatase crystalline phase showed a significant improvement in the photocatalytic properties of the prepared samples, which was evaluated by studying their efficiency towards Rhodamine B dye degradation. Additionally, the effect of doping titania nanotubes with noble metals (e.g. Ag, Pt, and Au), or covering their surface with noble metal nanoparticles, was studied regarding their capabilities towards the photocatalytic degradation of Rhodamine B dye. A positive effect when samples were doped with Ag was revealed.

*Keywords: doped titania nanotubes, photocatalysis, dye degradation.*

## INTRODUCTION

For many years the process of anodic oxidation of titanium (Ti) in different electrolytes has been studied due to its potential in obtaining nanostructured titanium dioxide (TiO$_2$). This material is of great interest for many applications, such as solar energy conversions in Gratzel-type solar cells [1–3], as photocatalyst [4–7], including reactions of water electrochemical splitting (photoelectrolysis) [8–10], as an active material in gas sensors [11, 12], as well as in several biomedical applications [13, 14]. A key factor in many of those applications is the possibility of producing a nanostructured material with predetermined shapes, like porous structures, tubes, or spheres. These structures present a large active surface in a very small volume, which contributes to the enhancement of their physical and optical properties. Therefore, nanostructured TiO$_2$ is considered one of the most efficient, low-cost, and highly stable photocatalysts. Nevertheless, the main drawbacks of this material are its wide bandgap and high recombination rate of charge carriers. One way of overcoming these shortcomings is to produce porous materials doped with catalytic metals, which would enhance the photocatalytic properties of TiO$_2$ nanostructures.

The key processes responsible for both the anodic formation of nanoporous titanium dioxide structures and growing matrices of TiO$_2$ nanotubes seem to be the same. They are determined by the metal oxidation and the pore growth controlled by the chemical dissolution of the oxide produced under a given potential difference.

Titania nanotubes are also of especial interest as future platforms to be used as nanoengines, autonomous entities, which perform a controlled motion in the presence of certain fuels or external stimuli [15–20]. While the first potential tubular nano- and micromotors were generally moving in the presence of hydrogen peroxide and showed great potentialities as microtransporters [21–27] and many other sensing and environmental applications [28, 29], their usage has been highly restricted by the toxic nature of the hydrogen peroxide fuel. One of the most interesting alternatives for the mentioned fuel has been the light-induced microengines, whose movement is promoted by a renewable energy source, and the reactions involved do not generally generate waste products. In addition to all advantages of such a motion principle, titania structures are inherently biocompatible, which makes them the perfect candidates for drug delivery in the human body and for other biological applications.

In this regard, the investigation of photocatalytic properties of TiO$_2$ nanotubes and the related mechanisms, including the study of nanotubes doped with catalytic metals, is of special importance not only for their future implementation as microengines but also for their potential implementation in environmental issues related to the photocatalytic decomposition of various pollutants of interest.

In this paper we describe the influence of thermal treatment, doping, and deposition of noble metal nanoparticles on the arrays of titania nanotubes prepared by anodic oxidation, in addition to the photo-

catalytic activity of such structures with respect to the degradation of Rhodamine B under UV-light.

## PREPARATION OF TUBULAR TIO$_2$ NANOTEMPLATES

Ti foils (Sigma-Aldrich) with the thickness of 0.25 mm and purity of 99.7% were used in electrochemical experiments to prepare porous titanium dioxide structures. The samples were degreased in acetone and methanol in an ultrasound bath, followed by washing in deionized water and drying under nitrogen flow before anodic oxidation.

A mixture of hydrofluoric acid (48%), ethylene glycol, and phosphoric acid (H$_3$PO$_4$) in the ratio of 0.95:110:11 ml, respectively, was used for the electrochemical oxidation procedure. The experiments were carried out at room temperature. The Ti foil samples were attached to a Cu support by means of silver paste and mount in a three-electrode electrochemical cell with a Pt-electrode, used as a cathode, while the sample was subjected to electrochemical treatment as an anode, and a Ag/AgCl (1M KCl) electrode was used as a reference electrode. The applied voltage between the working electrode and the reference electrode, as well as the anodic oxidation current, were measured by using a Keithley digital multimeter. A Vegatescan TS5130MM scanning electron microscope (SEM) equipped with an EDX detector was used for sample characterization in terms of morphology and composition.

The oxygen transfer in organic electrolytes is much more difficult compared to that in aqueous electrolytes, which reduces the rate of oxide formation. Therefore, the oxide-reduction process due to the ionic exchange is accelerated in presence of water by the small thickness and the low quality of the formed barrier layer. The incorporation of organic components as electrolytes in the oxide film formation leads to a decrease of the relative permittivity of the layer, contributing to an increase of the breakdown voltage [30]. A high breakdown voltage of the oxide in anhydrous electrolytes ensures a larger range of anodic oxidation voltages, inducing the creation of nanotubular membranes.

The applied voltage was gradually increased at a rate of 1V/s till reaching the value of 120V. Subsequently, that voltage was maintained for different periods of time. The application of a gradually increased voltage ensures the formation of seeds, around which nanotubes are formed afterwards.

Au, Ag, and Pt were initially deposited on Ti foil for the fabrication of doped TiO$_2$ nanomembranes. The deposition was performed by using a Cressington 108 Sputter Coater in a cathodic arc plasma process, achieving the thickness of 500 nm of the catalytic metal films on three different Ti foils. The thicknesses of the deposited metal films can be precisely controlled by the deposition time. The foils with the deposited metal film were subsequently subjected to thermal treatment under Ar atmosphere at 950°C during 2 hours to promote the diffusion of the catalytic metal into the Ti foil substrate. As a result, TiO$_2$ layers doped with Au, Ag, or Pt were formed on the surface of the substrate. Moreover, arrays of TiO$_2$ nanotubes were obtained on the mentioned foils by means of electrochemical treatment, as described above. Figure 1 presents SEM images of the obtained TiO$_2$ layers.
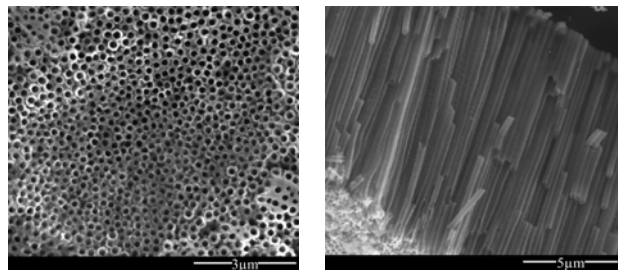


**Fig. 1.** SEM images of TiO$_2$ layers produced by anodic oxidation.

However, so as to produce metal nanodots onto the surface of TiO$_2$ nanotube arrays it is necessary to apply different experimental conditions. Fifty nm of Au, Ag, or Pt films were deposited on the surfaces of preliminarily produced TiO$_2$ nanotube arrays to obtain such metal nanostructures. Afterwards the samples were annealed at 500°C to form metal nanodots on the surface of TiO$_2$ nanotubes arrays. The synthesis of metal nanodots is due to the surface tension created during this process, which also promotes the crystalline phase transition from amorphous to anatase structure. It is necessary to mention that annealing at 500°C is enough for the formation of nanodots on the surface of TiO$_2$ nanotubular structure, as illustrated in Fig. 2. One can not subject the produced TiO$_2$ nanotubes to annealing at 950°C, since annealing at temperatures higher than 800°C leads to the formation of a rutile structure with a lower photocatalytic activity. Moreover, upon annealing at 950°C, the tubular structure is deformed.
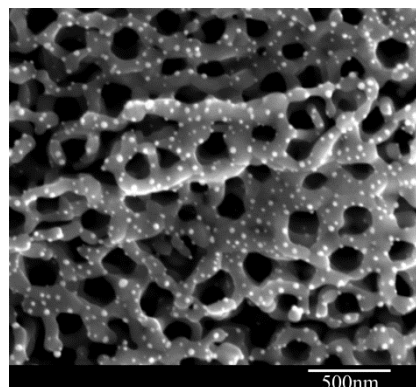


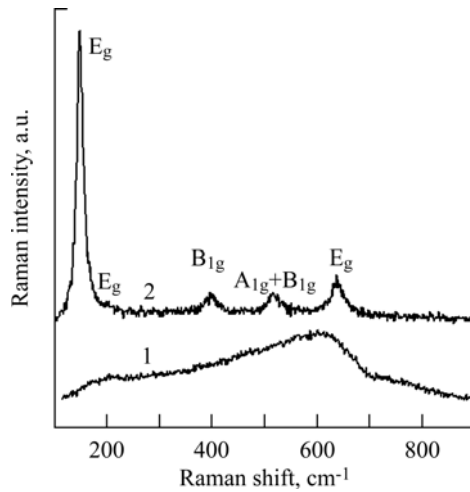**Fig. 2.** SEM images of TiO$_2$ nanotubes covered by catalytic metal nanoparticles.

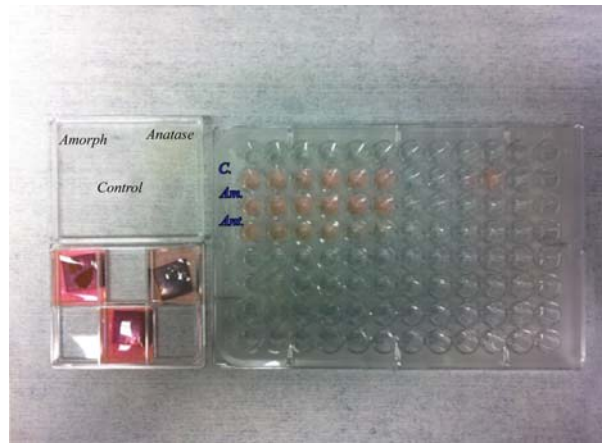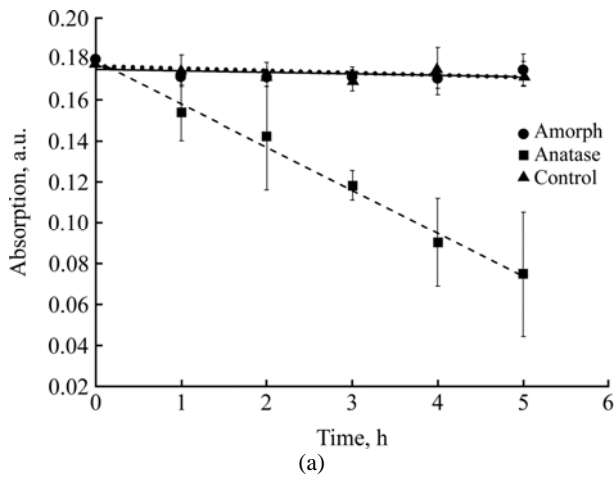**Fig. 3.** Raman spectra of TiO$_2$ nanotubes as prepared (1) and after being subjected to annealing at 500°C (2).



**Fig. 4.** Photocatalytic activity of TiO$_2$ nanotubes. (a) Photodegradation of Rhodamine B by TiO$_2$ nanotubes under UV-light after 5 hours exposure; (b) Image of samples after being exposed to UV-light during 5 hours.
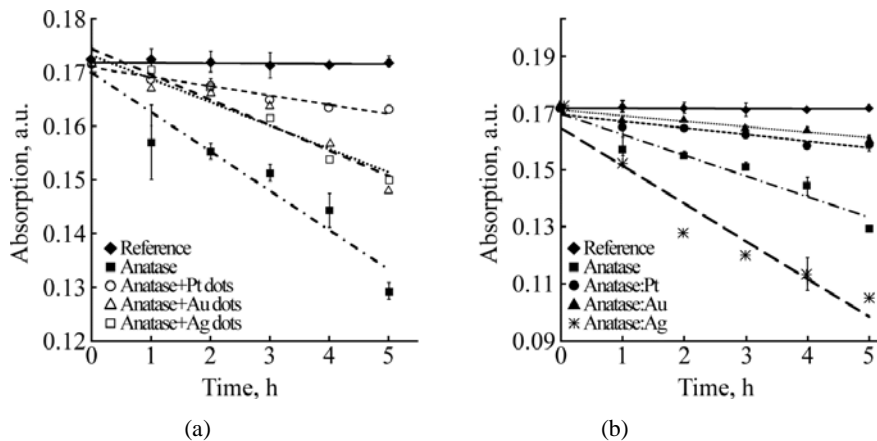


**Fig. 5.** Dependence of absorption upon exposure time for samples with anatase structure doped with Au, Ag, or Pt (a); and for samples covered by metal nanodots (b).

The transition from amorphous to the anatase state upon thermal treatment at 500°C is demonstrated by the Raman scattering analysis, as shown in Fig. 3.

The analysis of Fig. 3 suggests that as prepared TiO$_2$ nanotubes are amorphous, while those annealed at 500°C have an anatase crystalline structure. Anatase is tetragonal, with two TiO$_2$ formula units (six atoms) per primitive cell. The space group is $D_{4h}^{19}$ (I4/amd). There are 15 optical modes for this structure: $1A_{1g} + 1A_{2u} + 2B_{1g} + 1B_{2u} + 3E_g + 2E_u$. Three modes are infrared active, namely, the $A_{2u}$ mode and the two $E_u$ modes. The $B_{2u}$ mode is silent. The remaining six modes corresponding to symmetries $A_{1g} + 2B_{1g} + 3E_g$ are Raman active. The Raman shift for these phonons is 514 cm$^{-1}$ for the $A_{1g}$ mode, 399 cm$^{-1}$ and 514 cm$^{-1}$ for the $B_{1g}$ modes, and 144 cm$^{-1}$, 197 cm$^{-1}$ and 639 cm$^{-1}$ for the $E_g$ modes

[31]. Therefore, the $A_{1g}$ and one of the $B_{1g}$ modes overlap.

## INVESTIGATION OF TUBULAR TIO$_2$ PHOTOCATALYTIC PROPERTIES

The photocatalytic properties of the produced samples have been evaluated by studying the Rhodamine B degradation under UV in the presence of 1 mg of TiO$_2$ nanotubes. The initial concentration of Rhodamine B was $10^{-6}$ M, while the illumination source used in such experiments was a LAX-Cute Xenon Light Source 100 W ultraviolet lamp. A fixed volume from each sample has been taken from the solution each hour to perform spectrophotometric studies and to evaluate their absorption at the wavelength of 550 nm. The photodegradation of Rhodamine B by the photocatalytic activity of TiO$_2$ with different crystalline phases is shown in Fig. 4a. A significant photocatalytic activity is observed only for the anatase crystalline phase.

The photodegradation of Rhodamine B, assessed from the decrease of optical absorption, is only appreciable in the case of nanostructured TiO$_2$ sample with the anatase crystalline phase. The absorption values do not practically change upon 5 hours of exposure in the case of the control sample (no nanostructured TiO$_2$ is present in the mixture) or the amorphous nanostructured TiO$_2$ sample. The sample with the anatase structure becomes almost transparent upon 5 hours of exposure to UV-light, while the pink color of the control and of the amorphous samples does not practically change upon irradiation.

The results of investigations concerning the efficiency of Rhodamine B degradation for TiO$_2$ arrays doped with catalytic metals or covered by metal nanoparticles are shown in Fig. 5. The results are compared with those of the control samples (rhombic symbols) as well as with those of the TiO$_2$ undoped samples (square symbols). One can easily realize that there is dye degradation in both doped and nanodot covered samples. However, certain enhancement of the photocatalytic activity regarding Rhodamine B degradation is observed only for the TiO$_2$ nanotube arrays doped with Ag, while doping with Au and Pt, as well as covering of samples with any nanoparticles of Ag, Au, or Pt, leads to a decrease of photocatalytic activity.

It is known that doping or covering of TiO$_2$ samples with noble metals alters their photocatalytic activity. Of special importance are the photoreaction conditions kept during the experiment, as well as the methods and conditions of sample preparation [32]. The effects of doping upon photocatalytic properties can be described in the following terms: (i) an enhancement of the electron–hole separation by acting as electron traps and improving the charge transfer, (ii) an extension of the light absorption into the visible range and an enhancement of the surface electron excitation due to the excitation of plasmon resonances, (iii) a modification of surface properties of the photocatalyst, (iv) blocking the reaction sites on the TiO$_2$ surface, (v) passivation of the photocatalyst surface. While the first two effects should improve the photocatalytic properties, the last three can significantly decrease the photocatalytic activity. Therefore, one can conclude that the first two effects prevail in our samples doped with Ag, while the negative effects are predominant in the samples doped with Pt or Au, as well as in samples covered by metal nanoparticles. However, it is not excluded that the optimization of other technological conditions may lead to a positive result for all of the samples.

## CONCLUSIONS

The results obtained in the present study demonstrate that thermal treatment of TiO$_2$ nanotube arrays prepared by anodic oxidation of titanium foils at 500°C leads to the transformation of the as-prepared amorphous nanotubular structure to a crystalline anatase phase, which leads to an enhancement of the photocatalytic activity towards the degradation of Rhodamine B dye. Doping of anatase TiO$_2$ nanotubes with Ag further improves the photocatalytic properties, while doping of samples with Pt or Au, as well as covering with metal nanodots, was found to have a negative impact on the rate of photocatalytic degradation of Rhodamine B. However, with the corresponding optimization of technological conditions, other positive results related to doping of TiO$_2$ nanostructures by other noble metals could probably be obtained. Additionally, a high photocatalytic activity shown by the anatase crystalline structures developed in the present work suggests their possible biological application as microengines moved by means of the UV-light, as well as their usage in sensors or as useful tools for environmental purposes.

## ACKNOWLEDGEMENTS

## REFERENCES

1. Uchida S., Chiba R., Tomiha M., Masaki N. and Shira M. Application of Titania Nanotubes to a Dye-sensitized Solar Cell. *Electrochemistry* 2002, **70**(6), 418–420.

2. Adachi M., Murata Y., Okada I. and Yoshikawa S. Formation of Titania Nanotubes and Applications for Dye-sensitized Solar Cells. *J. Electrochem. Soc.* 2003, **150**(8), 488–493.

3. Frank A.J., Kopidakis N., Lagemaat J. Electrons in Nanostructured TiO$_2$ Solar Cells: Transport, Recom-

7

bination and Photovoltaic Properties. *Coordin. Chem. Rev.* 2004, **248**(13–14), 1165–1179.

4. Adachi M., Murata Y., Harada M. and Yoshikawa S. Formation of Titania Nanotubes with High Photocatalytic Activity. *Chem. Lett.* 2000, **29**(8), 942–944.

5. Chu S.Z., Inoue S., Wada K., Li D., Haneda H. and Awatsu S. Highly Porous $(TiO_2-SiO_2-TeO_2)/Al_2O_3/TiO_2$ Composite Nanostructures on Glass with Enhanced Photocatalysis Fabricated by Anodization and Sol−Gel Process. *J. Phys. Chem. B* 2003, **107**(27), 6586–6589.

6. Zhang H., Zhao H., Zhang S., Quan X. Photoelectrochemical Manifestation of Photoelectron Transport Properties of Vertically Aligned Nanotubular $TiO_2$ Photoanodes. *Phys. Chem.* 2008, **9**(1), 117–123.

7. Kontos A.G., Kontos A.I., Tsoukleris D.S., Likodimos V., Kunze J., Schmuki P., Falaras P. Photo-induced Effects on Self-organized $TiO_2$ Nanotube Arrays: the Influence of Surface Morphology. *Nanotechnology* 2009, **20**(4), 045603–045612.

8. Mor G.K., Shankar K., Varghese O.K., Grimes C.A. Photoelectrochemical Properties of Titania Nanotubes. *J Mater. Res.* 2004, **19**(10), 2989–2996.

9. Lakshminarasimhan N., Bae E., Choi W. Enhanced Photocatalytic Production of $H_2$ on Mesoporous $TiO_2$ Prepared by Template-free Method: Role of Interparticle Charge Transfer. *J. Phys. Chem. C* 2007, **111**(42), 15244–15250.

10. Mor G.K., Prakasam H.E., Varghese O.K., Shankar K., Grimes C.A. Vertically Oriented Ti-Fe-O Nanotube Array Films: Toward a Useful Material Architecture for Solar Spectrum Water Photoelectrolysis. *Nano Lett.* 2007, **7**(8), 2356–2364.

11. Varghese O.K., Gong D., Paulose M., Ong K.G., Grimes C.A. Hydrogen Sensing using Titania Nanotubes. *Sensor Actuat. B-Chem.* 2003, **93**(1–3), 338–344.

12. Manno D., Micocci G., Rella R., Serra A., Taurino A. and Tepore A. Titanium Oxide thin Films for $NH_3$ Monitoring: Structural and Physical Characterizations. *J. Appl. Phys.* 1997, **82**(1), 54–59.

13. Oh S.H., Finõnes R.R., Daraio C., Chen L.H., Jin S. Growth of Nano-scale Hydroxyapatite using Chemically Treated Titanium Oxide Nanotubes. *Biomaterials* 2005, **26**(24), 4938–4943.

14. Tsuchiya H., Macak J.M., Mueller L., Kunze J., Müller F., Greil P., Virtanen S., Schmuki P. Hydroxyapatite Growth on Anodic $TiO_2$ Nanotubes. *J. Biomed. Mater. Res.* 2006, **77**(3), 534–541.

15. Mei Y., Huang G., Solovev A.A., Ureña E.B., Mönch I., Ding F., Reindl T., Fu R.K.Y., Chu P.K., Schmidt O.G. Versatile Approach for Integrative and Functionalized Tubes by Strain Engineering of Nanomembranes on Polymers. *Adv Mater.* 2008, **20**(21)**,** 4085–4090.

16. Gao W., Sattayasamitsathit S., Orozco J., Wang J. Highly Efficient Catalytic Microengines: Template Electrosynthesis of Polyaniline/Platinum Microtubes. *J. Am. Chem. Soc.* 2011, **133**(31), 11862–11864.

17. Gao W., Pei A., Wang J. Water-Driven Micromotors. *ACS Nano* 2012, **6**(9), 8432–8438.

18. Gao W., Uygun A., Wang J. Hydrogen-Bubble-Propelled Zinc-Based Microrockets in Strongly Acidic Media. *J. Am. Chem. Soc.* 2012, **134**(2), 897–900.

19. Hong Y., Diaz M., Córdova-Figueroa U.M., Sen A. Light-Driven Titanium-Dioxide-Based Reversible Microfireworks and Micromotor/Micropump Systems. *Advanced Funct. Mater.* 2010, **20**(10), 1568–1576.

20. Giudicatti S., Marz S.M., Soler L., Madani A., Jorgensen M.R., Sanchez S., Schmidt O.G. Photoactive Rolled-up $TiO_2$ Microtubes: Fabrication, Characterization and Applications. *J. Mater. Chem. C.* 2014, **2**(29), 5892–5901.

21. Sanchez S., Solovev A.A., Schulze S., Schmidt O.G. Controlled Manipulation of Multiple Cells using Catalytic Microbots. *Chem. Commun.* 2011, **47**(2), 698–700.

22. Kagan D., Campuzano S., Balasubramanian S., Kuralay F., Flechsig G.-U., Wang J. Functionalized Micromachines for Selective and Rapid Isolation of Nucleic Acid Targets from Complex Samples. *Nano Lett.* 2011, **11**(5), 2083–2087.

23. Orozco J., Campuzano S., Kagan D., Zhou M., Gao W., Wang J. Dynamic Isolation and Unloading of Target Proteins by Aptamer-modified Microtransporters. *Anal. Chem.* 2011, **83**(20), 7962–7969.

24. Garcia M., Orozco J., Guix M., Gao W., Sattayasamitsathit S., Escarpa A., Merkoci A., Wang J. Micromotor-based Lab-on-chip Immunoassays. *Nanoscale* 2013, **5**(4), 1325–1331.

25. Balasubramanian S., Kagan D., Jack Hu C.-M., Campuzano S., Lobo-Castañon M.J., Lim N., Kang D.Y., Zimmerman M., Zhang L., Wang J. Micromachine-Enabled Capture and Isolation of Cancer Cells in Complex Media. *Angew. Chem. Int. Edit.* 2011, **50**(18), 4161–4164.

26. Campuzano S., Orozco J., Kagan D., Guix M., Gao W., Sattayasamitsathit S., Claussen J.C., Merkoçi A., Wang J. Bacterial Isolation by Lectin-modified Microengines. *Nano Lett.* 2011, **12**(1), 396–401.

27. Soler L., Magdanz V., Fomin V.M., Sanchez S., Schmidt O.G. Self-Propelled Micromotors for Cleaning Polluted Water. *ACS Nano.* 2013, **7**(11), 9611–9620.

28. Kagan D., Calvo-Marzal P., Balasubramanian S., Sattayasamitsathit S., Manesh K.M., Flechsig G.-U., Wang J. Chemical Sensing Based on Catalytic Nanomotors: Motion-Based Detection of Trace Silver. *J. Am. Chem. Soc.* 2009, **131**(34), 12082–12083.

29. Wu J., Balasubramanian S., Kagan D., Manesh K.M., Campuzano S., Wang J. Motion-based DNA Detection using Catalytic Nanomotors. *Nature Commun.* 2010, **1**(36), 1–6.

30. Foll H., Langa S., Carstensen J., Christophersen M. and Tiginyanu I.M. Pores in III–V Semiconductors. *Adv. Mater.* 2003, **15**(3), 183–198.

31. Ohsaka T., Izumi F. and Fujiki Y. Raman Spectrum of Anatase $TiO_2$. *J. Raman Spectrosc.* 1978, **7**(6), 321–324.

32. Anpo M. and Kamat P.V. *Environmentally Benign Photocatalysts: Applications of Titanium Oxide-based Materials.* New York, Dordrecht, Heidelberg, London: Eds, Springer, 2010. 757 p.

## Реферат

Массивы нанотрубок диоксида титана были получены путем анодного окисления титановой фольги в растворе электролита, содержащего смесь фтористо-водородной кислоты, этиленгликоля и фосфорной кислоты. При термообработке при 500°C, первоначально аморфные нанотрубки кристаллизуются в нанотрубки с фазой Анатаз. Нанотрубки с кристаллической фазой Анатаз показали значительное улучшение фотокаталитических свойств полученных образцов, которые оценивались путем изучения их эффективности с деградаций красителя Родамина Б. Кроме того, эффект легирования нанотрубок диоксида титана благородными металлами (то есть Ag, Pt и Au), или покрытия их поверхности благородными металлическими наночастицам, был изучен в отношении их способностей к фотокаталитической деградации Родамина Б. Был выявлен положительный эффект легирования образцов Ag.

*Ключевые слова: легированные нанотрубки диоксида титана, фотокатализ, деградация красителей.*